Available online at www.sciencedirect.com
ScienceDirect
Journal of Power Sources 159 (2006) 291–294
JOURNAL OF POWER SOURCES
www.elsevier.com/locate/jpowsour

Short communication

Synthesis and characterization of $LiNi_{0.8}Co_{0.2}O_2$ as cathode material for lithium-ion batteries by a spray-drying method

H.M. Wu, J.P. Tu *, X.T. Chen, Y.F. Yuan, Y. Li, X.B. Zhao, G.S. Cao

Department of Materials Science and Engineering, Zhejiang University, Hangzhou 310027, China

Available online 5 June 2006

Abstract

Layered structure $LiNi_{0.8}Co_{0.2}O_2$ cathode material for lithium-ion batteries was synthesized by sintering the precursor, which was obtained from the corresponding metal acetate solution via a spray-drying method. The structure, morphology and reaction mechanism of the powders were characterized by means of XRD, SEM and TG-DTA. The electrochemical properties of the $LiNi_{0.8}Co_{0.2}O_2$ cathode were also investigated by using a coin-type cell containing Li metal as the anode in a potential range of 3.0–4.3 V. Upon sintering the spray-dried powders at 750 °C for 24 h, the $LiNi_{0.8}Co_{0.2}O_2$ particles obtained are fine, narrowly distributed and well crystallized. As a result, the synthesized $LiNi_{0.8}Co_{0.2}O_2$ has excellent electrochemical properties. The simple synthesis procedure is time and energy saving, and thus is promising for commercial application.

Keywords: $LiNi_{0.8}Co_{0.2}O_2$; Spray-drying method; Lithium-ion batteries; Electrochemical characteristics

1. Introduction

Lithiated metal oxides, having the layered α-$NaFeO_2$ structure, have been extensively studied as cathodes in rechargeable lithium batteries. Only $LiCoO_2$ compound has been widely used as a cathode material in commercial lithium-ion battery production successfully. But due to its high cost and toxicity, many efforts have been made to replace $LiCoO_2$. Another attractive candidate is $LiNiO_2$ for its low cost and its possibility of a high charge/discharge capacity. However, $LiNiO_2$ also has a few disadvantages compared to $LiCoO_2$. Its major disadvantages are the difficulty in preparation so as to achieve stoichiometry and poor cycle life [1–4]. Now, an appealing alternative that alleviates the disadvantages of both $LiCoO_2$ and $LiNiO_2$ is the solid solution $LiNi_xCo_{1-x}O_2$ [5,6].

Recently, extensive studies have been devoted to fabricate the $LiNi_xCo_{1-x}O_2$ material through solid-state processes [7,8], sol–gel methods [9,10], co-precipitation routes [11] and reverse-microemulsion route [12]. By all these methods, the target materials have been synthesized successfully and exhibited better electrochemical characteristics compared to $LiNiO_2$ cathode material.

Spray-drying method is an excellent synthetic powder technology [13,14]. By this method, ultrafine $LiCoO_2$ [15], submicron sized $LiMn_2O_4$ [16] and spherical $Li_{1+x}V_3O_8$ [17] have previously been synthesized successfully. In this work, layered $LiNi_{0.8}Co_{0.2}O_2$ powders are obtained after sintering the precursor prepared by the spray-drying method. The structure and morphology of the precursor and synthesized $LiNi_{0.8}Co_{0.2}O_2$ powders are investigated. Also the electrochemical properties of the layered $LiNi_{0.8}Co_{0.2}O_2$ compound as the positive electrode material are studied.

2. Experimental

Stoichiometric amounts of $CH_3COOLi{\cdot}2H_2O$, $Co(CH_3COO)_2{\cdot}4H_2O$ and $Ni(CH_3COO)_2{\cdot}4H_2O$ were dissolved in distilled water. The resulting solution was dried to form a mixed dry precursor via a spray-dryer. The solution was atomized via a sprinkler at an air pressure of 0.2 MPa, and was dried in the spray-dryer by dry hot air. The inlet air temperature was 220 °C, and the exit air temperature was 110 °C. The as-prepared precursor was annealed at 500 °C in air for 4 h. Then the obtained powder were ground in an agate mortar and re-annealed at 750 °C for 24 h under flowing oxygen to obtain the product.

DTA and TG were carried out on an analyzer (TA SQT600) with a heating rate of 10 °C min^{-1} in the temperature range of 50–900 °C. Powder X-ray diffraction (XRD, Rigaku D/max-rA)

* Corresponding author. Tel.: +86 571 87952573; fax: +86 571 87952856.
E-mail address: tujp@cmsce.zju.edu.cn (J.P. Tu).

0378-7753/$ – see front matter © 2006 Elsevier B.V. All rights reserved.
doi:10.1016/j.jpowsour.2006.04.032

was used to analyze the phase of the sintered powders. The morphology of the powders was observed with a field emission scan electron microscopy (FESEM, FEI SIRION JY/T010-1996).

A slurry consisting of the sintered powder as active material, conducting agent (acetylene black), and binder (polyvinylidene fluoride) was pasted onto an aluminum foil, with *N*-methylpyrrolidone (NMP) as the solvent. The weight ratio of active material, conducting agent and binder was 80:10:10 in the working electrode. After drying in air at 80 °C for 4 h, the sheet was pressed under a pressure of 20 MPa to provide increased adherence of the cathode mixture onto the aluminum foil current collector. The weight of active material in the electrode sheet was about 10.0 mg in a square centimeter of aluminum foil. After drying in a vacuum at 120 °C for 10 h, the electrodes were assembled into the coin-type cells (CR 2025) in an Ar-filled glove box. The metallic lithium sheet was used as the counter electrode. A solution of 50 vol.% ethylene carbonate (EC), 50 vol.% dimethyl carbonate (DMC) and 1 M $LiPF_6$ was used as the electrolyte solution, and a polypropylene (PP) film (Cellgard 2300) as the separator. The galvanostatic charge-discharge tests were conducted on a PCBT-138-8D-A battery program-control test system with the cut-off voltages of 3.0 and 4.3 V (versus Li/Li^+) at a specific current density of 10 mA g^{-1}. The cyclic voltammetry measurements were performed on a CHI604B electrochemical workstation at room temperature with a scan rate of 0.1 mV s^{-1}. Electrochemical impedance spectrum (EIS) measurements were also carried out on this instrument. The cells for impedance measurements were performed on discharged states completely and relaxed for 24 h over the frequency-range 100 kHz–1.0 mHz at a potentiostatic signal amplitude of 10 mV.

3. Results and discussion

TG and DTA traces by thermal analysis of the precursor powders obtained by spray-drying method are shown in Fig. 1. Several prominent heat events (endotherms and exotherms) are observed. The strong endothermic peak at about 100 °C is related to the release of water. On TGA curves, the initial weight loss of about 10% is accompanied. During 160–300 °C, no apparent weight loss is found, but on DTA curves, small endothermic and exothermic peaks could also obviously observed. Maybe in this process, the reactions do not involve weight loss. Combining the results of TG and DTA, it is found that the second continuous weight loss accompanying the complex endotherms and exotherms is nearly complete around 500 °C, which accounts for about 50% of the initial weight loss in TG and corresponds to three sharp endothermic peaks at 340, 360 and 420 °C. This step corresponds to the decomposition of metal acetate and the formation of $LiNi_{0.8}Co_{0.2}O_2$ gradually. Above 500 °C, the weight of sample hardly changes. It mainly associates the $LiNi_{0.8}Co_{0.2}O_2$ crystallization. At higher temperature, the small weight loss is due to the loss of lithium in the compound. Therefore, the selected heating treatment process is that, firstly, at relative low temperature, $LiNi_{0.8}Co_{0.2}O_2$ powders are synthesized; secondly, good crystallization is obtained at elevated temperature.

The XRD pattern of $LiNi_{0.8}Co_{0.2}O_2$ compounds prepared by a spray-drying method following sintering at 750 °C for 24 h is shown in Fig. 2. The pattern can be indexed to a single phase of the α-$NaFeO_2$ type with space group *R*3*m* and shows very sharp peaks, indicating a high degree of crystallinity. The diffraction peaks show a clear splitting of the hexagonal characteristic doublets (0 0 6)/(1 0 2) and (1 0 8)/(1 1 0), indicating that the product has the typical layered characteristic. The intensity ratio of *I* (0 0 3) peak to *I* (1 0 4) peak is about 1.53 and the lattice parameters *a*- and *c*-axis are about 2.874 and 14.217 Å, respectively. So the *c*/*a* ratio is 4.95, which is in the range of the characteristic value of α-$NaFeO_2$ layered structure.

Fig. 3 shows a SEM image of the sample morphology. The particle size of the sample, prepared by spray-drying method, is small and homogeneous, which consists of submicron (200–300 nm) particles whose crystalline facets are relatively well-defined. Moreover, it is obviously observed that the conglomeration takes place among particles.

The electrochemical behaviors of $LiNi_{0.8}Co_{0.2}O_2$ powders prepared in this work were characterized by cyclic voltammograms with coin cell. As shown in Fig. 4, the voltage was scanned from 3.0 to 4.3 V, and then backed to 3.0 V with a scan rate of

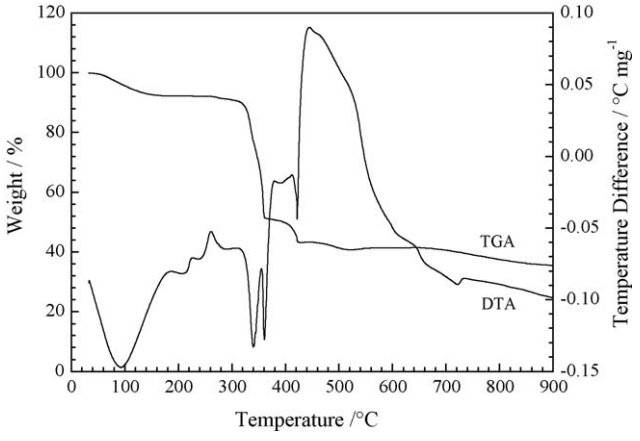

Fig. 1. TG/DTA curves of the precursor powder prepared by spray-drying method.

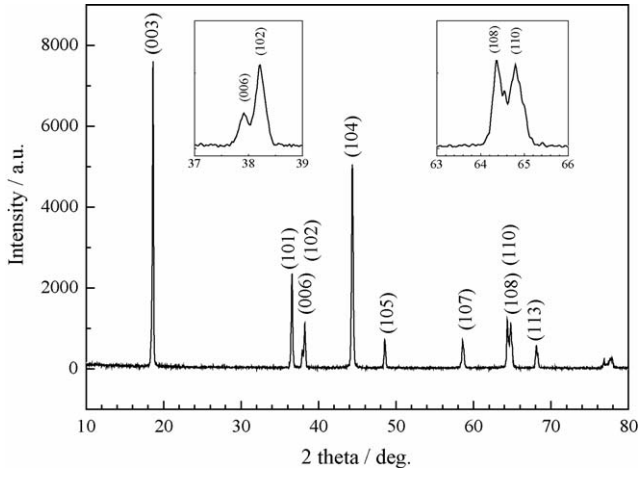

Fig. 2. The XRD pattern of layered $LiNi_{0.8}Co_{0.2}O_2$ compound prepared by spray-drying method.

Fig. 3. A SEM image of $LiNi_{0.8}Co_{0.2}O_2$ powders.

$0.1\ mV\ s^{-1}$. It is shown that the shape of first cyclic voltammograms is very different from that of next cyclic voltammograms. At the first cycle, the oxidation peak at about 4.25 V is found, while the oxidation peak is observed at 3.90 V at the next cycles. Moreover, the corresponding peak current at the next cycle is only the half for the first cycle. However, at different cycles, all the corresponding reduction peaks are found at about 3.6 V. It indicates that the lithium insertion/extraction in $LiNi_{0.8}Co_{0.2}O_2$ is reversible, and also the most irreversible capacity arises in the first cycle.

Fig. 5 shows the charge/discharge profiles of $LiNi_{0.8}Co_{0.2}O_2$ compound prepared by spray-drying method between 3.0 and 4.3 V at a current density of $10\ mA\ g^{-1}$. In agreement with the CV features, both of the charging and discharging curves of $LiNi_{0.8}Co_{0.2}O_2$ shows only one voltage plateau, respectively, but the charge plateau is higher than that of the discharge. As shown in Fig. 5, the material exhibits high cyclic reversibility with a limited discharge capacity loss. The first charge and discharge capacities of the powders are 192 and $176\ mAh\ g^{-1}$, respectively. The Coulombic efficiency is 91%. It is found that the discharge capacities increase slightly in the initial stage and reaches a steady state after the fifth cycle, which is the highest discharge capacity of $180\ mAh\ g^{-1}$, probably because the $LiNi_{0.8}Co_{0.2}O_2$ powders in the cathodes are not thoroughly wetted at the first cycle. Once the intercalation and de-intercalation process start, the volume of the composite cathode begin to expand and shrink, enabling the electrolyte to wet the powders more thoroughly. After 5 cycles, the discharge capacity fades gradually. Till 20 cycles, the capacity still keeps a high value of $172\ mAh\ g^{-1}$.

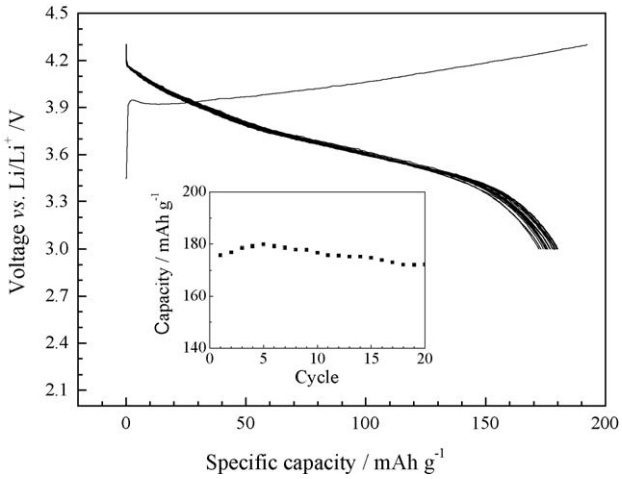

Fig. 5. First charge and the next discharge curves of $LiNi_{0.8}Co_{0.2}O_2$ electrode within the voltage range 3.0–4.3 V. The inset shows the corresponding cycling stability.

To investigate the electrode resistance changes during the cycle process, EIS tests were carried out and the Nyquist plots collected after the electrodes had undergone the desired cycles. The Nyquist plot evolutions are indicated in Fig. 6. Each of the impedance spectra includes three parts: a semicircle at the high frequencies reflects the resistance for Li^+ ion migration through the surface film and film capacitance; another semicircle at medium to low frequencies reflects charge-transfer resistance and interfacial capacitance between the electrodes and electrolyte; and the sloping line at very low frequencies reflects Li^+ ion diffusion in the solid state electrodes [18]. From Fig. 6, it is obvious that the diameter of the second semicircle is much

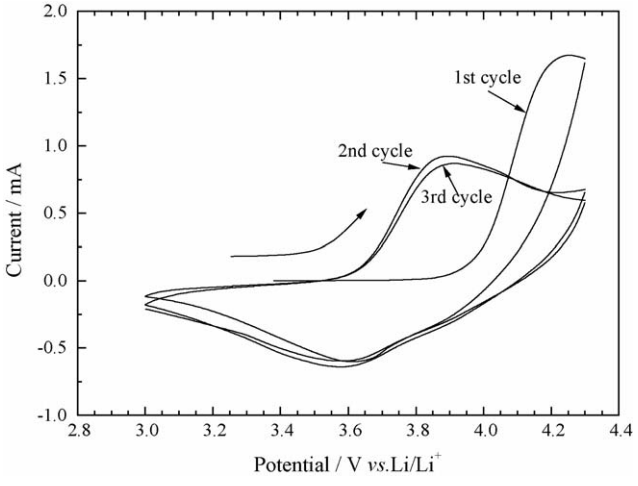

Fig. 4. Cyclic voltammogram for $LiNi_{0.8}Co_{0.2}O_2$ electrode with a scan rate of $0.1\ mV\ s^{-1}$.

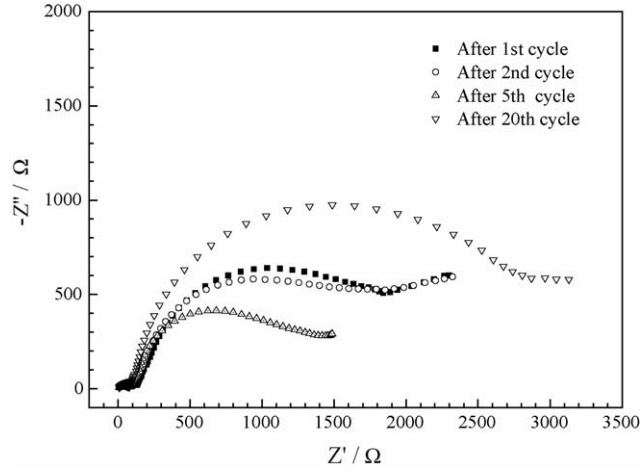

Fig. 6. Nyqusit plots of $LiNi_{0.8}Co_{0.2}O_2$ electrodes after different cycles.

larger than that of the first one, indicating that the charge-transfer resistance and interfacial capacitance between the electrodes and electrolyte is the major contributor to the total electrode resistance. It is clear from this figure that a pronounced difference appears after different cycles about the second semicircle. The diameter of second semicircle diminishes gradually. After 5 cycles, the diameter of that becomes the smallest, which can be understood that the discharge capacity reaches the highest. With increasing cycle number, the diameter enlarges drastically. At the 20th cycle, as indicated in Fig. 6, the diameter of the semicircle is larger than that of the first cycle, which may be the reason for the discharge capacity fading.

4. Conclusion

$LiNi_{0.8}Co_{0.2}O_2$ powders were prepared by a spray-drying method and studied as the cathode material for lithium ion batteries. The material was obtained by re-annealing the powders in oxygen after annealing the precursor in air. The sub-micro size products had a layered structure. At room temperature, the material delivered a capacity of 176 mAh g^{-1} at the first cycle in the charge/discharge voltage range of 3.0–4.3 V. During the charge and discharge process, the discharge capacity increased slightly in the initial stage. After reached the highest capacity at the fifth cycle, the capacity faded gradually. At 20 cycles, the capacity sustained a value of 172 mAh g^{-1}.

References

[1] M. Okada, K.-I. Takahashi, T. Mouri, J. Power Sources 68 (1997) 545.
[2] Y. Nitta, K. Okamura, K. Haraguchi, S. Kobayashi, A. Ohata, J. Power Sources 54 (1995) 511.
[3] C. Pouillerie, L. Croguennec, P. Biensan, P. Awillmann, C. Delmas, J. Electrochem. Soc. 147 (2000) 2061.
[4] C. Nayoze, F. Ansart, C. Laberty, J. Sarrias, A. Rousset, J. Power Sources 99 (2001) 54.
[5] M.A. Señarís-Rodríguez, S. Castro-García, A. Castro-Couceiro, C. Julien, L.E. Hueso, J. Rivas, Nanotechnology 14 (2003) 277.
[6] C. Delmas, I. Saadoune, Solid State Ionic 53–56 (1992) 370.
[7] A. Ueda, T. Ohzuku, J. Electrochem. Soc. 141 (1994) 2010.
[8] J. Cho, G. Kim, H.S. Lim, J. Electrochem. Soc. 146 (1999) 3571.
[9] C.-C. Chang, N. Scarr, P.N. Kumta, Solid State Ionic 112 (1998) 329.
[10] R.V. Chebiam, F. Prado, A. Manthiram, J. Electrochem. Soc. 148 (2001) A49.
[11] J. Cho, B. Park, J. Power Sources 92 (2001) 35.
[12] C.-H. Lu, H.-C. Wang, J. Mater. Chem. 13 (2003) 428.
[13] F. Iskandar, L. Gradon, K. Okuyama, J. Colloid Interface Sci. 265 (2003) 296.
[14] K. Okuyama, I.W. Lenggoro, Chem. Eng. Sci. 58 (2003) 537.
[15] Y.X. Li, C.R. Wan, Y.P. Wu, C.Y. Jiang, Y.J. Zhu, J. Power Sources 85 (2000) 294.
[16] C.Y. Wan, Y. Nuli, Q. Wu, M.M. Yan, Z.Y. Jiang, J. Appl. Electrochem. 33 (2003) 107.
[17] J. Gao, C.Y. Jiang, C.R. Wan, J. Power Sources 125 (2004) 90.
[18] H. Liu, Z. Zhang, Z. Gong, Y. Yang, Solid State Ionic 166 (2004) 317.